Molecular Crystals and Liquid Crystals
Publication details, including instructions for authors and subscription information:
http://www.tandfonline.com/loi/gmcl20

Preparation of Indium Tin Oxide Inks for Electrically Conductive Transparent Oxide Film with Ink-Jet Printing Method

JeJeong Yu [a], Sungkoo Lee [a], Eunhee Lim [a], TaeHo Kim [b] & Kyeong K. Lee [a]

[a] Green Chemistry & Manufacturing System Division, Korea Institute of Industrial Technology (KITECH), Chonan-Si, Korea

[b] Department of Polymer Engineering, Sungkyunkwan University, Suwon, Korea

Version of record first published: 19 Apr 2010

To cite this article: JeJeong Yu, Sungkoo Lee, Eunhee Lim, TaeHo Kim & Kyeong K. Lee (2010): Preparation of Indium Tin Oxide Inks for Electrically Conductive Transparent Oxide Film with Ink-Jet Printing Method, Molecular Crystals and Liquid Crystals, 519:1, 134-140

To link to this article: http://dx.doi.org/10.1080/15421401003609848

Mol. Cryst. Liq. Cryst., Vol. 519: pp. 134–140, 2010

ISSN: 1542-1406 print/1563-5287 online
DOI: 10.1080/15421401003609848

Preparation of Indium Tin Oxide Inks for Electrically Conductive Transparent Oxide Film with Ink-Jet Printing Method

JEJEONG YU,[1] SUNGKOO LEE,[1] EUNHEE LIM,[1] TAEHO KIM,[2] AND KYEONG K. LEE[1]

[1]Green Chemistry & Manufacturing System Division, Korea Institute of Industrial Technology (KITECH), Chonan-Si, Korea
[2]Department of Polymer Engineering, Sungkyunkwan University, Suwon, Korea

*The ink-jet printing method is an important process in display industry due to the low-cost production of large-scale electronic devices. In this work, we prepared the nanoparticle indium tin oxide (ITO) solutions for ink-jet printing and characterized the electrical, structural and morphological properties of the film. The improvement of conductivity after reduction process was correlated with the sharpening of the diffraction peak as proved by X-ray diffraction measurement. The ITO inks was coated on a glass by spin-coating process and patterned by the ink-jet printing technique using a 50 μm diameter ink-jet nozzle. The sheet resistance and optical transmission of ITO thin film was ca. 50∼300Ω/sq and ca. 75∼95%, respectively. The electrical resistance of patterned ITO lines showed about 5∼30 * 10^3Ω. The detailed relationship between microstructure and properties are discussed.*

Keywords Colloid; indium tin oxide; ink-jet; nanoparticle

1. Introduction

Because of its high transmittance, good electrical conductivity, excellent substrate adherence, hardness and chemical inertness, Indium tin oxide (ITO) thin films are extensively used in anti-static coatings, heat reflecting mirrors, solar cells, flat panel display device, liquid crystal displays, electroluminescent devices etc. [1–3]. ITO is an n-type semiconductor with a band gap between 3.5 eV and 4.3 eV and a maximum charge carrier concentration in the order of $10^{21}\,cm^{-3}$ [1–2]. A number of the manufacturing techniques for depositing the ITO thin film have been utilized by vacuum evaporation, chemical vapor deposition (CVD), electron beam deposition, sputtering, spray pyrolysis and sol-gel process [1–4]. The advantages of ink-jet printing include easy scalability, low cost production, flexibility of pattern formation

Address correspondence to Kyeong K. Lee, Green Chemistry & Engineering Department, KITECH, 35-3 Hongchon-ri, Ipchang-Myun, Seobuk-gu, Cheonan-Si, Chungnam, Korea. E-mail: klee45@kitech.re.kr

over the conventional vacuum deposition processes which involve the costly photolithographic process [5]. In this work, we describe the synthetic procedure of ITO nanoparticles with wet chemical process. And we discuss structural properties, surface morphologies and the electrical and optical characterization results of the ITO thin films. And we demonstrate the direct pattern formation of ITO thin lines with ink-jet printing method.

2. Experimental

2.1. *Preparation of Indium Thin Oxide(ITO) Powder*

For the synthesis of ITO nanoparticles, we closely followed the procedure by R. Nonninger *et al.* given in [6]. All chemicals were used as received from the supplier. A mixture of 14 g of Indium(+III) chloride, 1.8 g of tin(+IV) chloride and 0.56 g of caprolactam were introduced into 140 ml of deionized-water in a round bottom flask. After continuous stirring, an opalescence reaction mixture solution turned into a clear solution. Then the solution mixture was heated to 50°C. After this temperature had been reached, 10.5 ml of ammonium hydroxide solution were added dropwise, with an additional vigorous stirring for 24 hours. For complete precipitation, a further 28 ml of ammonium hydroxide solution were subsequently added to the mixture. A white precipitate of indium oxide hydroxide was formed in the bottom of the flask, which was centrifuged off (30 min at 4000 rpm). The powder was dried at 190°C in a vacuum drying cabinet until slight yellowing of the powder was observed. The dried powder was finely mortared, distributed in crystallizing dishes and placed in a forming gas oven. The oven was evacuated, then flooded with nitrogen. The oven was heated up to 250°C with a heating rate of 250°C/hour under a nitrogen flow rate of 200 L/hour. This temperature was maintained for 60 minutes under forming gas atmosphere with a gas flow rate of 300 L/hour. Thereafter, the oven cooled down under nitrogen atmosphere until it reached room-temperature. This resulted in a dark blue powder which was identifiable as pure indium oxide phase by means of X-ray diffraction analysis.

2.2. *Coating Solution and Film Formation*

a) ITO Coating Solution. A turbo mill was charged with ITO powders and a mixture solution (acid: 3,6,9-trioxadecanoic acid/base: TMAH). And the turbo milling was carried out for 3 hours. Subsequently, this milled ITO suspensions were homogenized for 10 minutes for a uniform dispersion with a carrying medium solvent. Again, this suspension was centrifuged off for 5 min at 4000 rpm. After finishing centrifugation, the solutions were filtered through membrane filter with 1.0 μm pore size.

b) Film Formation. The soda lime float glasses had been used as the coating substrates. Before coating, the glass substrates were cleaned ultrasonically for 60 minutes in acetone, followed by ethanol rising, and then blow-dried with a nitrogen gun. ITO solution was coated on the substrate using a spin-coating process. After deposition, the films were underwent heat-treatment in nitrogen atmosphere in the range of 300–600°C for 30 min, and then cooled down to room-temperature under the nitrogen condition.

2.3. *Printed ITO Line by the Ink-Jet Printing Technology*

ITO ink was directly patterned on a glass by the ink-jet printing technique using a 50 μm diameter nozzle purchased from MicroFab Technology. Soon after the ITO ink-jet printing process, an intermediate curing of the pattern was performed on a hot-plate in air. The temperature of a heating stage during ink deposition was maintained in the range of 40∼80°C.

2.4. *Characterizations*

The thicknesses of the ITO thin films were measured by a depth profiler (KLA-Tencor Alpha-step IQ). The crystalline phases of the ITO thin films were determined by X-ray diffractometer (PROTO LXRD-MG40L) using Cu $K\alpha_1$ rays. The X-ray measurements on the ITO film were carried out with θ-2θ scan from 7° to 80° at a scanning rate of 3°/min. The sheet resistance values of the samples were measured by the four-point probe method at room temperature with Loresta-GP model MCP-T600. For the optical characteristic measurement of the ITO thin films were performed by UV–VIS spectrophotometer (in wavelength of 300–800 nm) with Shimadzu UV-2550. A scanning electron microscopy (SEM) was employed for the purpose of studying surface morphologies of ITO thin films by a JEOL FE-SEM(JSM 6701F).

3. Result and Discussion

3.1. *Structure of the ITO Powders*

The ITO powders that annealed at 250°C for 30 minutes in forming gas condition (8% of H_2 gas). The yellowed ITO powders were turned into blue powders after the forming gas treatments. Figure 1 compares before (a) and after (b) heat-treatment under the forming gas treatments along with before (c) and after (d) for the cases of the commercially obtained powders. Comparing the sharpness and narrowness of the diffraction peaks at (222), (400), (440), (622) designated in the figure, one can see that the crystal structures for both cases are clearly improved. All the peaks in the patterns can be indexed to In_2O_3 with cubic bixbyite crystal structure with referenced to JCPDS database (06-416) [6]. Also, the diffraction peak at 32.8° became distinctive after reduction process primarily due to distortion of crystal structure in cubic In_2O_3 lattice by removal of oxygen atoms [9]. Further analysis of crystal structure for these materials is in process.

3.2. *Electrical Property of ITO Thin Films*

We prepared the ITO inks with the different solid contents of 15, 25, 35, and 40% and with the different temperature treatments at 300, 400, 500, and 600°C. The sheet resistances of the films coated with solutions of solid content ca. 15% are decreased with the increased layer ($2.1 * 10^3$, $4.8 * 10^2$, $2.3 * 10^2\,\Omega/\square$ for 1, 3, 5 layer ITO film, respectively). According to the morphologies obtained by SEM in Figure 2, the inclusion of more elongated rod-like feature with the increased solid contents seems an indicative of the improved conductivity as revealed by four-point resistivity measurements. The true nature of these rod-like features is still under investigation. Table 1 summarizes the observed resistance improvement of the films prepared from

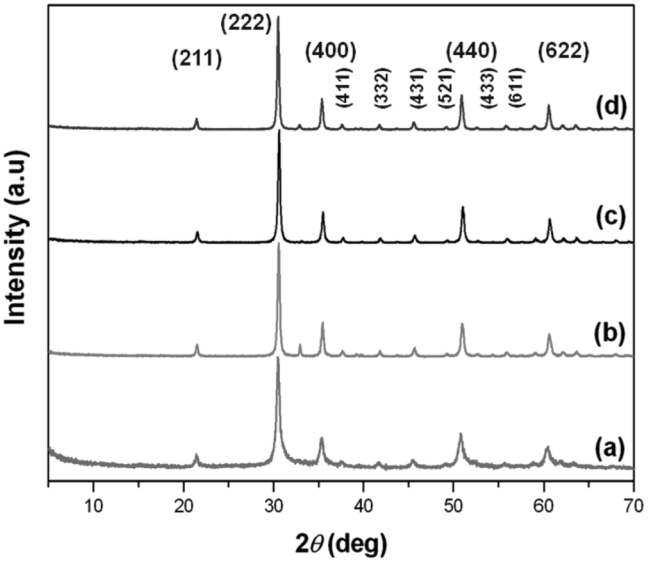

Figure 1. XRD patterns of ITO powders treated without forming gas, (a) and (c), and under forming gas environment, (b) and (d); (a) and (b) are from the synthesized ITO. (c) and (d) are from a commercially available ITO nanopowders.

particles before and after reduction process with forming gas treatments. It is known that the origin of electrical conductivity of ITO is due to oxygen vacancies in ITO lattice [11]. Since the hydrogen molecules in the forming gas bind to oxygen atoms in the ITO lattice under high temperature condition, in turn leading to oxygen vacancy states, the observed color changes of the powders might explain the improved conductivity of the films from the nanoparticles treated with forming gas [9,10]. Figures 3 and 4 show transmittance and sheet resistance are simultaneously decreased with the increasing solid content. It is known that higher transparency and lower resistivity have a reciprocal relationship to each other. High

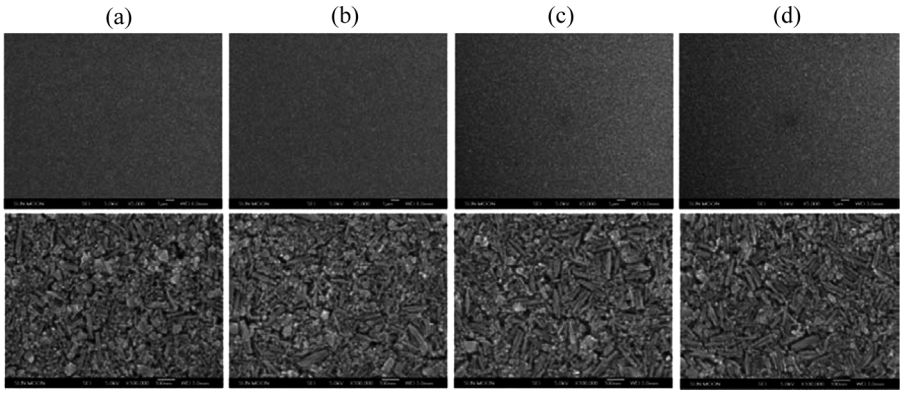

Figure 2. SEM images of ITO thin films containing different solid contents; (a) 15%, (b) 25%, (c) 35%, and (d) 40% (top pictures are magnified by 5,000 X and bottom pictures are magnified by 100,000 X).

Table 1. Conductivity comparison between ITO films before and after reduction using forming gas treatments

SAMPLE	Thickness (μm)	Resistance (Ω)	Sheet-resistance (Ω/□)
before reduction	1.02	130	585
after reduction	1.02	86.9	392

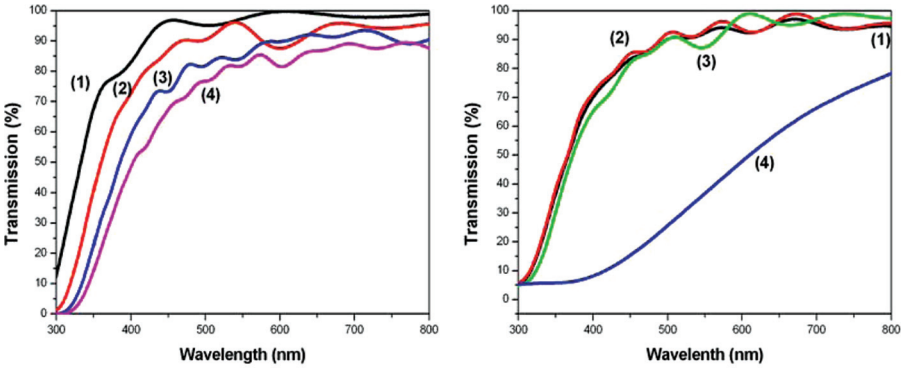

Figure 3. Transmittance of ITO thin films at various solid contents and annealing temperature. (a) (1)–(4) the solid contents were 15, 25, 35, and 40%, respectively. (heating temperature were 500°C) (b) (1)–(4): the heat – temperature were 300, 400, 500, and 600°C, respectively. (solid contents were 25%).

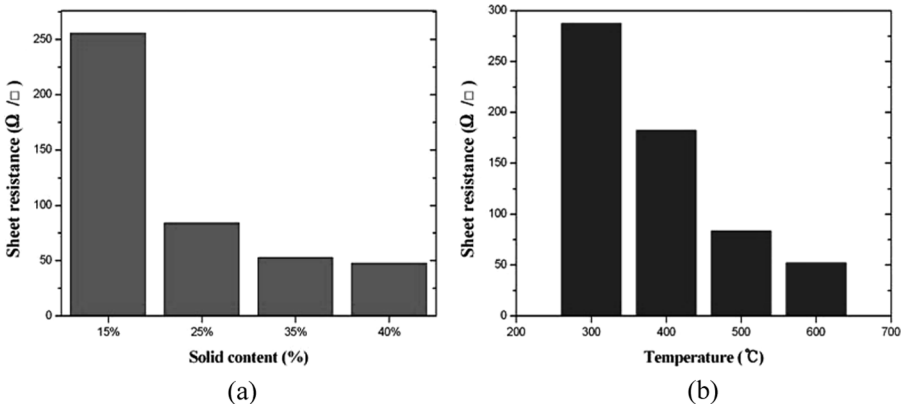

Figure 4. Sheet resistances of ITO thin films with various solid contents and with annealing temperature. (a) Sheet resistances of ITO thin films with different solid contents. (heating temperature were 500°C) (b) Sheet resistances of ITO thin films annealed at different temperatures (solid contents were 25%).

Table 2. The resistance of ITO pattern at different heating temperature. (Resistance measured with Keithley SCS-4200 semiconductor parameter analyzer. The probing distance was 1.0 mm

Heating Temperature (°C)	Thickness (μm)	Line length (μm)	Resistance (Ω)
25	1.012	83.19	$5.75768 * 10^4$
35	0.98011	71.75	$2.757442 * 10^4$
60	1.1726	80.07	$3.977938 * 10^4$
80	1.0765	79.55	$3.019968 * 10^4$

transmittance of above 80% maintained up to 500°C. But the transmittance is rapidly decreased when the film was annealed beyond 600°C, as proved by the morphology changes including creaks on the film [7–8].

3.3. *Ink-Jet Printed of ITO*

In order to prevent the clogging at the inkjet nozzle by the quick evaporation of the solvent in the ITO solution, the ITO solutions was further mixed with solvents, such as ethyleneglycol, having a higher boiling point than that of water. Table 2 shows the resistance of ITO lines patterned by Ink-jet process. Resistance was not widely changed with the increasing temperature but with the increasing temperature of heat stage. And the thickness was dramatically changed between the center and the edge of pattern. Figure 5 shows the morphologies of ITO lines patterned by ink-jet. The

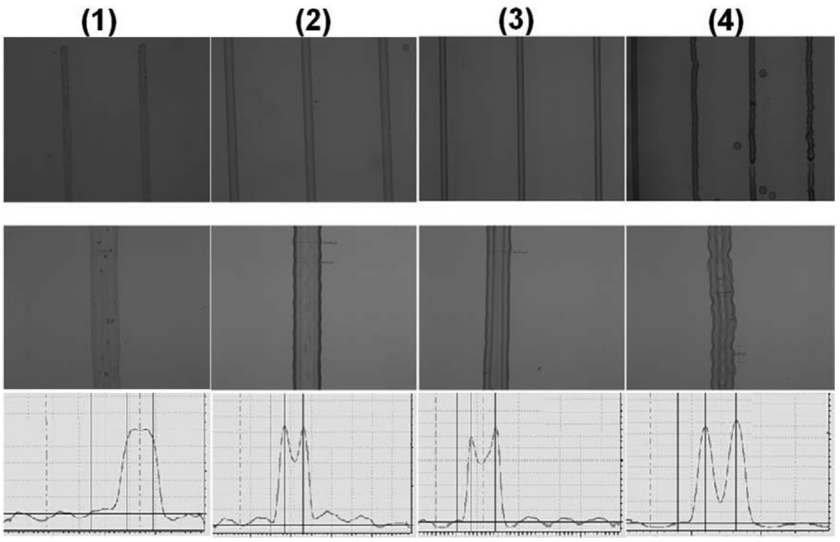

Figure 5. Optical images of ITO patterns with different temperature settings of heating-stage. During printing (1)–(4): The temperatures of the stage were 25, 35, 60, and 80°C, respectively. Top pictures from an optical microscope are magnified with 50 X and bottom pictures are magnified with 200 X.

shapes of ITO patterns observed are non-uniform across the edge of the patterned lines. By increasing temperature of heating-stage the thickness is rapidly changed between center and the edge of pattern because carrier solvent evaporates more quickly on the edge of a pattern than at the center of a pattern.

4. Conclusions

Colloidal ITO nanoparticle solutions are synthesized with a wet-chemical process for the preparation of ink-jettable inks. The structural, optical, electrical properties were discussed in relation with heat-treatment environment and solid-contents. The films coated with the nanoparticle solutions shows a rod-like features as the increment of solid-contents in the solutions. The rod-like features are closely related to the improvement in conductivity in the resultant ITO films. Also, we demonstrate that ITO lines can be patterned with ink-jet printing method.

Acknowledgement

This work has been developed under the support of The Next Generation New Technology Development Program by The Korean Ministry of Knowledge Economy.

References

[1] Liu, J., Gan, Y., & Zeng, S. (2006). *Surface and Coatings Tech.*, *201*, 25–29.
[2] Alam, M. J. & Cameron, D. D. (2000). *Thin Solid Films*, *00*, 455–459.
[3] Tomonaga, H. & Moromoto, T. (2001). *Thin Solid Films*, *392*, 243–248.
[4] Cho, Y. S., Kim, H. M., Hong, J. J., Yi, G. R., Jang, S. H., & Yang, S. M. (2009). *Colloids & Surfaces A: Physicochem. Eng.*, *336*, 88–98.
[5] Shim, G. H., Han, M. G., Sharp-Norton, J. C., Creager, S. E., & Foulger, S. H. (2008). *J. Mater. Chem.*, *18*, 594–601.
[6] Nonninger, R., Goebbert, C., Schmidt, H., Drumm, R., & Sepeur, S. US Patent 6553966 B1.
[7] Su, C., Sheu, T.-K., Chang, Y.-T., Wan, M.-A., Feng, N.-C., & Hung, W.-C. (2005). *Synthetic Metals.*, *153*, 9–12.
[8] Fallah, H. R., Ghasemi, M., & Hassanzadeh, A. (2007). *Physica E*, *39*, 69–74.
[9] Kim, K. Y. & Park, S. B. (2004). *Materials Chemistry and Physics*, *86*, 210–221.
[10] Tsai, M., Wang, C., & Hon, M. (2003). *Surface and Coatings Tech.*, *172*, 95–101.
[11] Frank, G. & Kostlin, H. (1982). *Appl. Phys. A: Solids Surf.*, *27*, 197.